

Validation of Goddard Earth Observing System-version 5 MERRA planetary boundary layer heights using CALIPSO

Nikisa S. Jordan,^{1,2} Raymond M. Hoff,^{1,2} and Julio T. Bacmeister³

Received 7 January 2010; revised 5 August 2010; accepted 12 August 2010; published 31 December 2010.

[1] This study compares the planetary boundary layer (PBL) height produced by the Goddard Earth Observing System-version 5 (GEOS-5) model with Cloud-Aerosol Lidar and Infrared Pathfinder Satellite Observations (CALIPSO). Part of GEOS-5 is an Atmosphere Global Circulation Model (GCM) used by National Aeronautics and Space Administration. Model developers are uncertain of the precision of model PBL height predictions since verification by direct observations of the PBL height is sparse. Validation of the PBL height serves as a diagnostic on whether the physics and dynamics packages are correct in the model. In this work, we report the global daytime PBL heights derived from dissertation work by Jordan (2009). We believe that this is the first large-scale observational study of PBL heights using CALIPSO. In this paper, we compare CALIPSO PBL heights to matched PBL heights from the GEOS-5 Modern Era Reanalysis for Research and Applications (MERRA) model. Extensive comparisons between the model output and satellite observations in the Western Hemisphere and over Africa gave model-measurement correlation coefficients (R) of 0.47–0.73. Comparisons have been performed for regions over land and water using clouds, aerosols, and mixed cloud-aerosol features to detect the PBL. The present study provides insight of regional PBL height variances in the GEOS-5 model. For much of the study region GEOS-5 predicts PBL heights within 25% of CALIPSO observations. A case over the Equatorial Pacific indicates that the GEOS-5/CALIPSO PBL height ratios exceed 1.25. PBL height biases in the Equatorial Pacific may be related to the GCM coupling scheme implemented in GEOS-5. Also, in some regions, the CALIPSO PBL heights are generally higher than the GEOS-5 model.

Citation: Jordan, N. S., R. M. Hoff, and J. T. Bacmeister (2010), Validation of Goddard Earth Observing System-version 5 MERRA planetary boundary layer heights using CALIPSO, *J. Geophys. Res.*, 115, D24218, doi:10.1029/2009JD013777.

1. Introduction

[2] National Aeronautics and Space Administration (NASA) has integrated a system of models to support climate studies and other Earth science research initiatives. The Data Assimilation System (DAS), known as the Goddard Earth Observing System-Version 5 (GEOS-5), includes a General Circulation Model (GCM) and analysis of observational sources of information [Rienecker *et al.*, 2008]. The goal is to build a unified modeling system for climate and weather applications. The first significant application of GEOS-5 has been the Modern Era Reanalysis for Research and Applications (MERRA) [Bosilovich, 2008]. MERRA was designed to examine the hydrologic

cycle [Bosilovich, 2008]. The retrospective analyses (or reanalyses) include a long-term continuous data record (statistics from 1979 to present day). This period encompasses the modern satellite observing era. One important diagnostic of MERRA is the performance of the planetary boundary layer (PBL), since it is one parameter that we can observe from space. Validation of the PBL height helps to diagnose the performance of the physics and dynamics packages in the climate model. The PBL is also a critical component in the Earth's climate system, because it defines the depth of the lowest layer of the atmosphere, which is defined by local heating, turbulence, and surface structure. A correct PBL height is necessary, for example, to give a good representation of low-level clouds in climate models. This is important since there are significant feedbacks between boundary layer clouds and climate [Arya, 1988, Stull, 1988, Stull, 2000]. The PBL also has a major influence on air quality forecasting. For example, incorrect forecasts of surface particulate matter (PM_{2.5}) and ozone concentrations, predicted by a chemical transport model might be attributed to inaccurate PBL estimates. This is because pollutants can be transported above

¹Joint Center for Earth Systems Technology, University of Maryland Baltimore County, Baltimore, Maryland, USA.

²Cooperative Center for Remote Sensing Science and Technology, NOAA-CREST Center, City College of New York, New York, USA.

³National Center for Atmospheric Research, Climate and Global Dynamics Division, Boulder, Colorado, USA.

the PBL and pollution concentrations increase at the surface when layers aloft mix down into the PBL. In stable air masses, pollutants can be trapped within the PBL which subsequently raises pollutant concentrations. Therefore, verification of PBL outputs from models is essential. However, it is difficult for modelers to assess the accuracy of the predicted PBL height due to sparse (in situ) global observations. Validation is especially important now since MERRA is now complete and available to the community along with other GEOS-5 analysis and forecast results [e.g., Moncrieff *et al.*, 2010; available online http://www.ucar.edu/yotc/documents/ip_090707.pdf].

[3] With recent advancement in remote sensing capabilities, PBL height determination is possible using data from active spaceborne lidar, which possesses the ability to view vast and remote areas on a regular basis. The aim of this present study is to use the attenuated backscatter coefficient from Cloud-Aerosol Lidar and Infrared Pathfinder Satellite Observations (CALIPSO) [Winker *et al.*, 2007], part of the A-Train satellite constellation, to obtain PBL heights and then compare those observations to the NASA GEOS-5 model outputs. The study was performed for August and December 2006. All CALIPSO PBL observations were averaged spatially and matched in space and time to compare with estimates from the GEOS-5 MERRA model.

[4] Satellite lidar data have been used to validate PBL estimates by models. Analysis of boundary layer height from Lidar In-space Technology (LITE) has been compared with PBL parameters in a climate model [Randall *et al.*, 1998]. The study by Randall *et al.* [1998] specifically compared PBL heights derived from LITE to a GCM and National Center for Atmospheric Research (NCAR) climate model. Results indicated that GCM PBL predictions were very close to the LITE-derived PBL retrievals, while the PBL heights from the NCAR climate model were generally 300–400 m lower than the satellite-derived estimate. GLAS (Geoscience Laser Altimeter System) data was used in the first global validation of the European Center for Medium-Range Weather Forecasts (ECMWF) forecast model [Palm *et al.*, 2005]. Palm found that the GLAS derived PBL height was 200–400 m higher over oceans than the model. However, there was an apparent correlation between the data sets on a global scale. CALIPSO, a satellite based lidar, has not been used to validate PBL depths estimated by models. This is the first hemispheric observational study of PBL heights using CALIPSO with comparisons to the GEOS-5 MERRA model. In order to avoid detection of nighttime residual layers that are not related to local heating at the time of the overpass, PBL height comparisons presented in this study were only derived from daytime data.

2. Data and Methods

[5] We compare PBL heights from the GEOS-5 model with PBL heights determined from CALIPSO global satellite measurements during 2 months, August 2006 and December 2006. These 2 months were chosen because CALIPSO data were only available after June 2006, the GEOS-5 output was available only for the 6 month period June to December 2006. However, the 2 months period

should capture the maximum change in the seasonal variations expected in boundary layer behavior.

2.1. GEOS-5 PBL Heights

[6] This study will examine PBL heights in the GEOS-5 data assimilation system (DAS). The GEOS-5 DAS is a state of the art system coupling a global atmospheric general circulation model (GEOS-5 AGCM) to NCEP's Grid-point Statistical Interpolation (GSI) analysis [Rienecker *et al.*, 2008]. The GEOS-5 DAS assimilates a variety of in situ and remotely sensed data. Ground-based observations from aircraft, radiosondes, and dropsondes are included. Satellite radiance data streams that are assimilated include TIROS Operational Vertical Sounders (TOVS), Earth Observing System (EOS) Aqua sounders, GOES Sounders, and Special Sensor Microwave Imagers (SSM/I) [Rienecker *et al.*, 2008]. Data corrections in the system are introduced via an Incremental Analysis Update (IAU) procedure [Bloom *et al.*, 1996] in which the corrections appear as forcing terms in the prognostic equations for the AGCM state variables. This procedure is known to minimize shocks to model physics as newly analyzed data is introduced every 6 h. In addition, forcing for the AGCM during the DAS cycle includes prescribed aerosols and radiatively active trace gases, sea surface temperature (SST), and sea ice. The Modern Era Reanalysis for Research and Applications (MERRA) [Rienecker *et al.*, 2008] is the first major application of the GEOS-5 DAS [Bosilovich, 2008].

[7] The PBL scheme employed in GEOS-5 uses the Lock *et al.* [2000] scheme for unstable layers and the Louis *et al.* [1982] scheme in stable shear driven regimes. Turbulent fluxes at a specific altitude depend on local gradients of the transported quantity, but the diffusion coefficient (K_{zz}) may depend on atmospheric properties at different levels. Non-local fluxes are not parameterized in GEOS-5. The final diffusion coefficient K_{zz} represents vertical mixing by all turbulent processes, including surface and cloud-top buoyancy production, and shear production.

[8] The quantity referred to as planetary boundary layer height (PBLH) in this study is found by examining vertical profiles of the K_{zz} . PBLH is diagnosed as the lowest model level for which K_{zz} falls below $1 \text{ m}^2/\text{s}$ when values above this threshold exist in the lowest two levels of the column. This threshold is somewhat arbitrary. It represents turbulent intensity roughly two orders of magnitude below typical peak values ($\sim 100 \text{ m}^2/\text{s}$) in a strongly convective model PBL. We use PBLH derived from K_{zz} profiles because it directly measures the extent of strong vertical mixing produced by the model's PBL parameterization, and is therefore the most useful height-like quantity to validate using the CALIPSO data. The GEOS-5 PBLH data used for this study is averaged over two 1800 s model physics time steps, i.e., hourly averages, on the AGCM's native two-dimensional $2/3^\circ \times 1/2^\circ$ longitude-latitude horizontal grid with 72 pressure levels extending to 0.01 hPa.

[9] It is worth emphasizing that only AGCM state variables (winds, temperature, humidity, and ozone) are directly assimilated, every 6 h. For 6 h intervals centered at analysis times, the GEOS-5 AGCM is run with incremental analysis update (IAU) corrections [Bloom *et al.*, 1996] to these state variables. During these intervals, PBL diffusivities

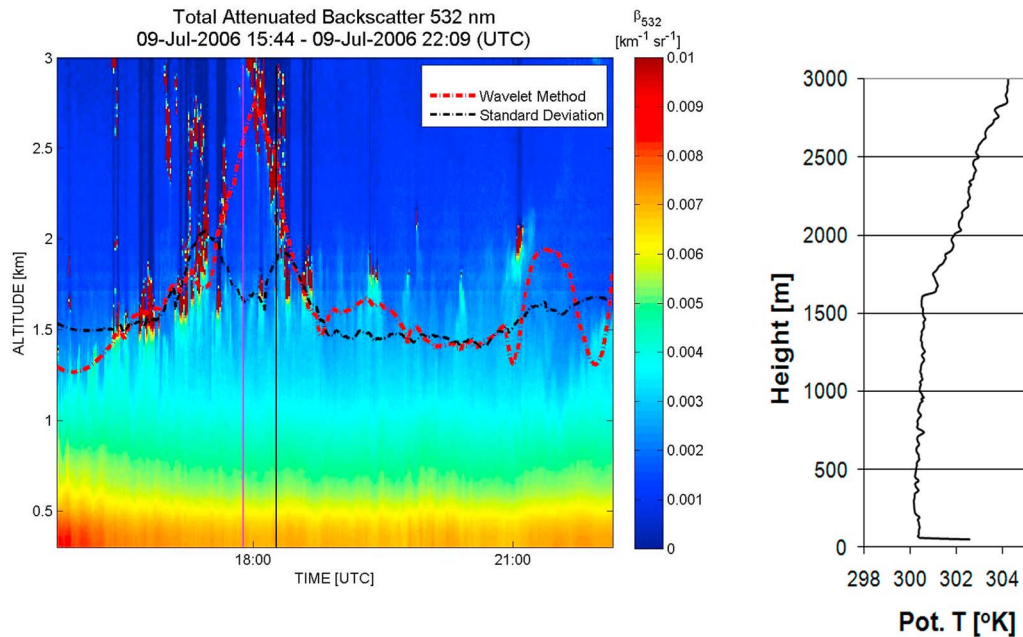


Figure 1. 9 July 2006 ELF ground-based lidar profile, with the PBL height via the maximum variance method (black dashed line) and Haar wavelet technique (red dashed line). The vertical fuchsia line is the coincidence between the radiosonde (26 km south of UMBC) potential temperature inversion at 1.64 km (shown on the right) and the ELF ground system PBLH, 1.60 km, derived from the maximum variance method at 17:51 UTC. The black vertical line corresponds to the closest point of approach (CPA \sim 60 km) of CALIPSO to ELF at 18:19 UTC. At that time the ELF PBLH determined by the variance method was \sim 1.70 km and CALIPSO was 1.60 km.

(and therefore heights) in the GEOS-5 DAS are produced by the AGCM physics routines at each 1800 s model physics time step exactly as they would be in a free running simulation.

2.2. PBL Heights From CALIPSO

[10] The CALIPSO payload includes (1) Cloud-Aerosol Lidar with Orthogonal Polarization (CALIOP), (2) an Imaging Infrared Radiometer (IIR), and (3) a moderate spatial resolution Wide Field Camera (WFC). All instruments operate separately and continuously. Together they provide information on the horizontal and vertical structure and properties of aerosols and clouds. CALIPSO is part of the afternoon (crosses the equator in the early afternoon \sim 1:30pm local time) A-Train constellation, which is a formation of several satellites flying in close proximity. This is of value since other satellites in the constellation can observe the same scene [Winker *et al.*, 2007]. Key characteristics of CALIOP are given by Winker *et al.* [2007, 2010].

[11] CALIOP is a three-channel (532 nm parallel, 532 nm perpendicular, 1064 nm) elastic lidar receiving light at the same wavelength as the emitted laser frequency. CALIOP sends short and intense pulses (1064 and 532 nm) of linearly polarized laser light downward towards Earth. The backscattered light is collected by the telescope receiver and is subsequently converted to an electronic signal. The atmospheric backscatter profile is retrieved at 30 m vertical

resolution from 0–8 km with a horizontal resolution of 333m.

[12] CALIPSO data are available from 13 June 2006 to present. The version 2 Level 1B (CAL_LID_L1-Prov-V2-01) data product was used in this study. A routine CALIPSO PBL product is currently not available. Methods used to derive the PBL height from CALIPSO are described by Jordan [2009]. Briefly, three separate methods have been evaluated: (1) a gradient technique [Melfi *et al.*, 1985; Boers and Eloranta, 1986; Palm *et al.*, 1998, 2005], (2) the Haar wavelet technique [Davis *et al.*, 2000; Brooks, 2003], and (3) a maximum variance technique, chosen here. Daytime lidar observations were used from CALIPSO to insure that residual layers were not picked out in nighttime data. Residual layers at night are most closely related to daytime maximum PBL heights and the matchup of the position of the PBL in daytime with a nighttime retrieval would needlessly complicate this analysis by having to compute transport over a 12 h period from a prior day PBL maximum. Daytime CALIPSO profiles have lower signal-to-noise ratio (SNR) than nighttime profiles due to the solar background reflected from clouds and the surface. This noise makes detection of a gradient in aerosol backscatter difficult because gradient techniques generally use some form of derivative calculation, which behaves poorly with noisy data. The second method employs a Haar wavelet [Cohn and Angevine, 2000], which assumes a structural form of the backscatter profile at the top of the PBL where the scattering has a strong increase just under the PBL (perhaps due to humidification of the aerosol),

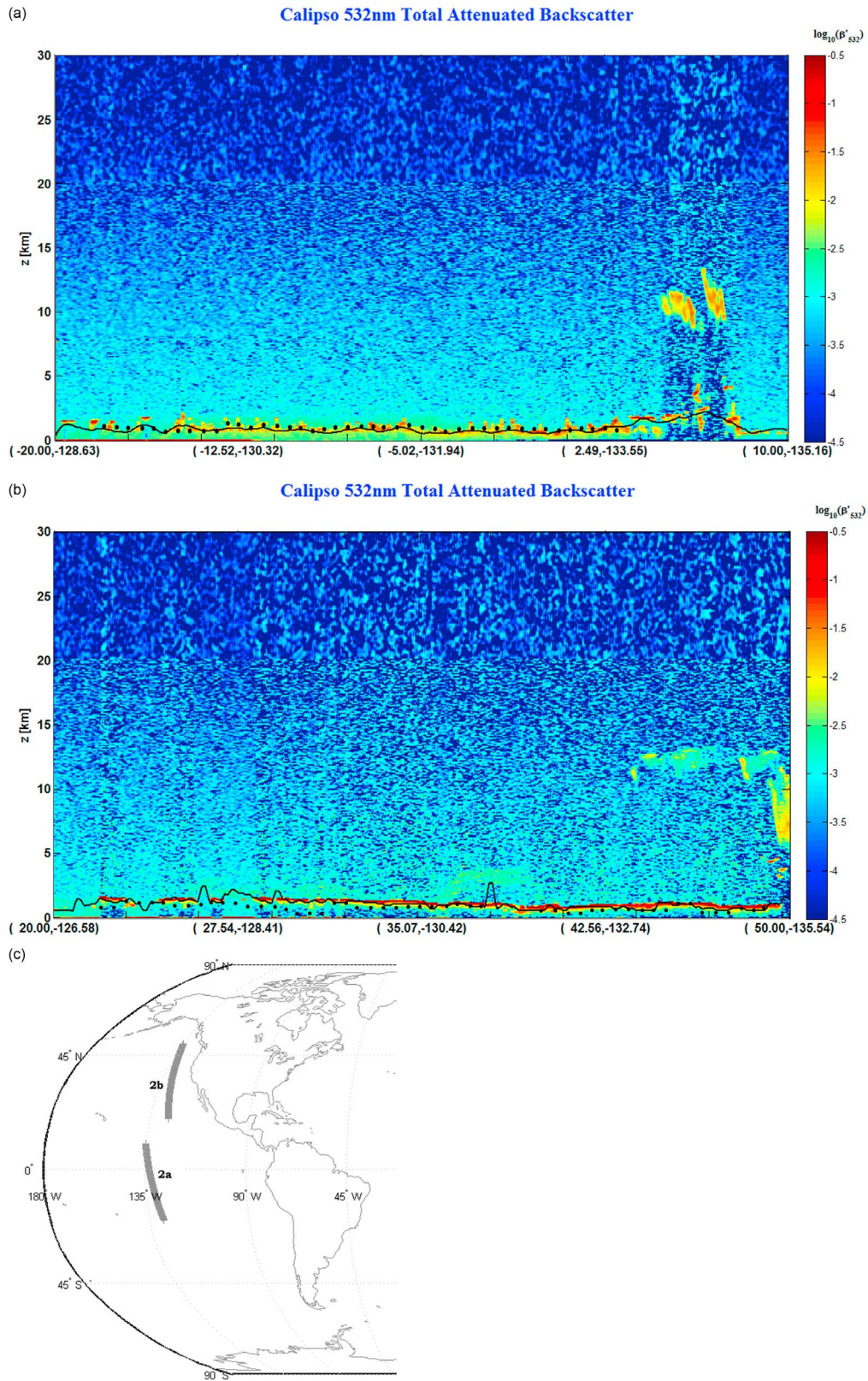


Figure 2

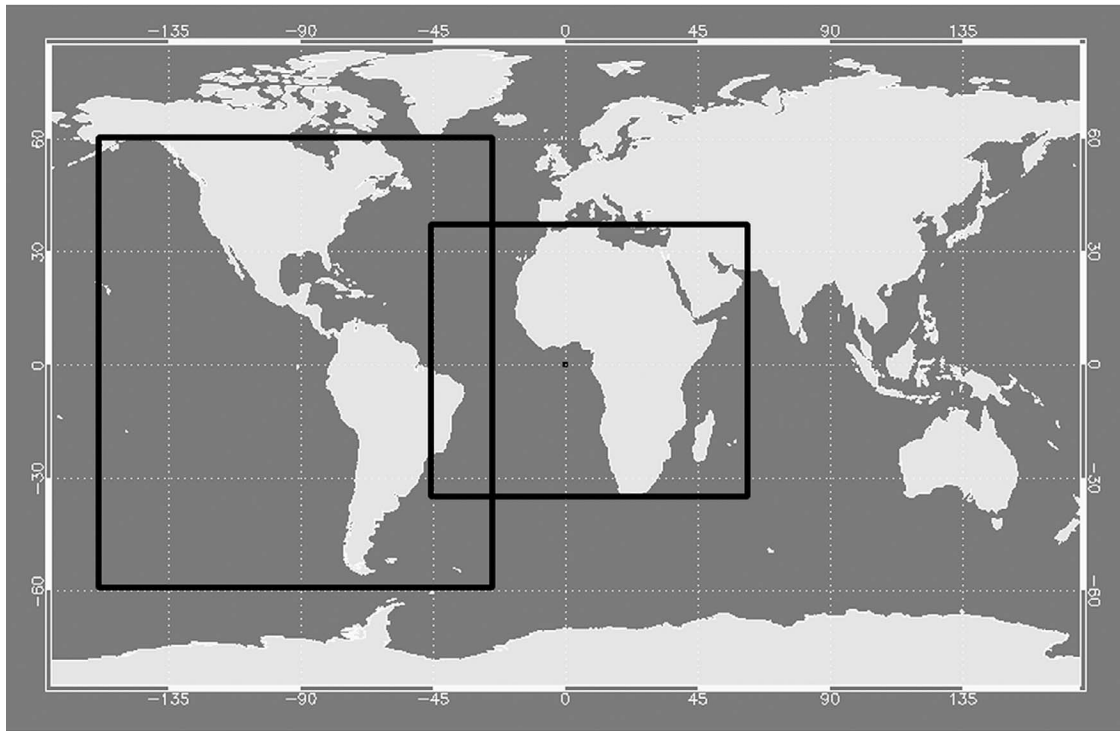


Figure 3. Study regions. (1) Western half of the globe (60.0°N , 60.0°S , 20.0°W , 160.0°W) and (2) Africa (35.0°N , 35.0°S , 45.0°W , 60.0°E).

a strong negative gradient of backscatter with height, and then a return to a constant or slowly decreasing backscatter coefficient above the PBL. This technique works reasonably well for a class of PBL structures which have high backscattering in the PBL peaking at the base of the inversion in the PBL followed by a detectable gradient in scattering and a lower backscattering above. The choice of the dilation (vertical scale) and magnitude (peak scattering) of the wavelet is more of an art than a science and it was found that the wavelet required more quality assurance than the third technique which is used here. The maximum variance technique is based on an idea by *Melfi et al.* [1985] which assumes that at the PBL there is a maximum in the variance of the backscatter signal both in the vertical dimension and in the horizontal dimension. Melfi used the technique with horizontal structures (rolls) in the cloud and aerosol field in over long horizontal flight paths with a downward looking lidar. We tested a similar technique from the ground where the assumption is that at the PBL, there is a maximum in the backscatter variance because within the entrainment region at the top of the PBL, downward clean eddies are mixing with upwelling hazier and higher backscatter parcels. If the entrainment zone is smaller or comparable to the region

over which we evaluate the variance in the signal, the peak variance in the vertical should identify the base of the entrainment zone since the absolute difference between the PBL value and the entrainment zone should be highest there, whether a peak in the signal due to aerosol swelling near the PBL top due to increased humidity or cloud base is seen or not. The use of variance (independent of the sign of the backscatter change) is more robust in clear air and partly cumulus convective cases. It was found for the noisy daytime CALIPSO data used here that the maximum variance technique with a sliding window best detected the PBL height (as evaluated visually by looking at the spatial latitude–height images from CALIPSO and in comparison with radiosoundings in the Baltimore–Washington area). Figure 1 shows such a comparison between a radiosounding with a very weak inversion in the potential temperature, the height of the PBL determined from both methods (2) and (3) from ground-based lidar at University of Maryland Baltimore County (UMBC; with a much higher SNR than CALIPSO) and a nearby CALIPSO retrieval using method (3). From this evaluation (including others with similar results but not shown here) [see *Jordan, 2009*], we chose to process the CALIPSO data set

Figure 2. (a) Attenuated backscatter plot of CALIPSO on 7 August 2006 at 22Z over the Eastern Pacific. (b) The CALIPSO overpass on 6 August 2006 at 22Z over the Pacific near the western United States. The derived PBLH is indicated with a solid black line with GEOS-5 PBLH indicated as black dots superimposed. Model PBL heights were higher (overall) than the satellite-derived estimate in Figure 2a and lower than the satellite PBL in some parts of Figure 2b. Figure 2c is the map showing the locations of the CALIPSO overpasses. It should be noted that these figures show the raw retrieved PBLH from the algorithm and that the final data used in the analysis has been filtered to remove cases where the algorithm failed along with elevated cloud features.

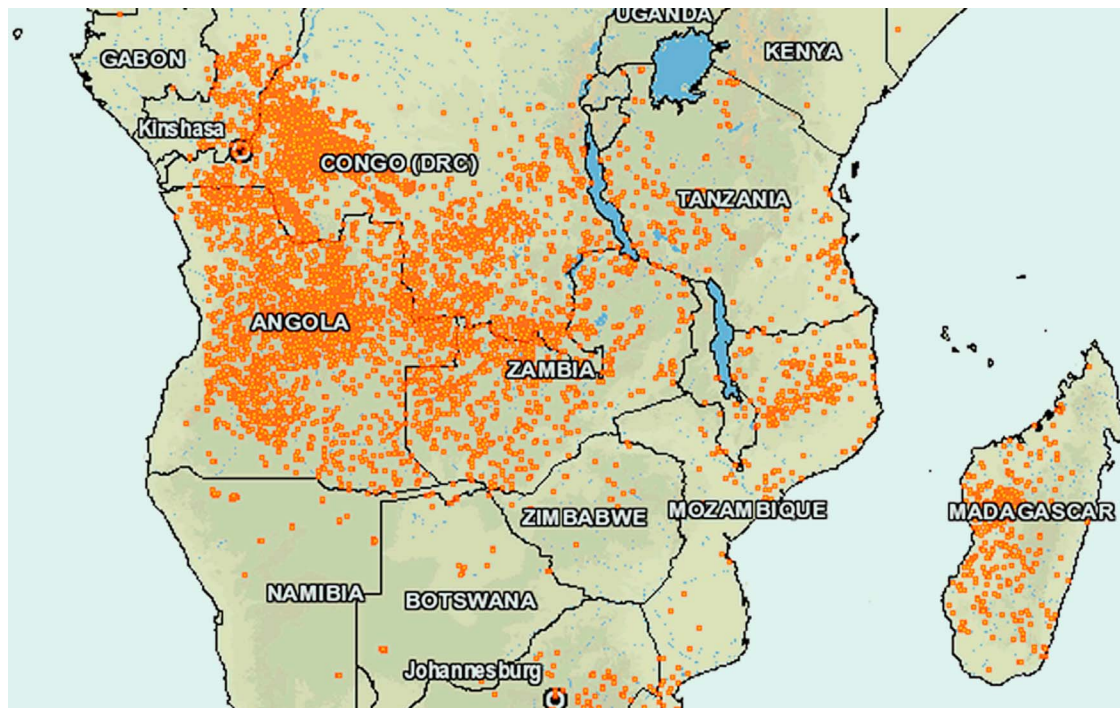


Figure 4. NASA Moderate Resolution Imaging Spectroradiometer (MODIS) active fire pixels (displayed as orange dots) for 18 August 2006 from FIRMS Web Fire Mapper. NASA/University of Maryland. (2002) MODIS Hotspot/Active Fire Detections. Data set. MODIS Rapid Response Project, NASA/GSFC [producer], University of Maryland, Fire Information for Resource Management System [distributors]. Available on-line [<http://maps.geog.umd.edu>].

using the maximum variance technique for PBL detection. Figures 2a and 2b are plots showing subsets of the derived CALIPSO PBL heights (variance technique (solid black line) before quality control) superimposed on the corresponding backscatter image with the GEOS-5 model PBL heights (shown as black circles). Figure 2a corresponds to a subset over the equatorial Pacific and Figure 2b is over the Pacific near the western United States. Further discussion regarding the variation between the satellite and model PBL heights is given in section 4. In that section ratio plots of the model estimate over the satellite observation are shown and provide a more comprehensive assessment of the differences in the data sets.

[13] The CALIPSO PBL data was flagged according to the feature type (i.e., aerosol, cloud, or both) used to derive it. The satellite and model data have different resolutions. Therefore, it is important to note that the satellite data was averaged to matchup to the model. As explained earlier, the model output is on a $2/3^\circ$ by $1/2^\circ$ longitude-latitude horizontal grid. Therefore, the CALIPSO PBL data was averaged (the mean was taken) every $1/2^\circ$ in latitude. Satellite and model data were then compared at the same time (within 30 min, where 30 min is the average time separation between model time step and the CALIPSO observation) and latitude and longitude. Model/satellite PBL height ratio maps were produced for all regions. Creating ratio plots was a great visual value since it made it easier to determine where the estimates were significantly different. Correlation plots of the model and satellite PBLs were created using the statistical software SAS

(Statistical Analysis System, 2009). Histogram charts were created as well to get a better understanding of the model and satellite PBL distributions.

3. Study Areas

[14] Possible matchups between CALIPSO and GEOS-5 were largely found in regions with few overlying cloud systems and clearly delineated PBL heights in the CALIPSO data. The predominance of such data occurs over the ocean. Therefore, a large portion of the Western Hemisphere was selected for comparisons. The area is bounded by the coordinates 60.0°N , 60.0°S , 20.0°W , and 160.0°W (Figure 3). Quality assurance via visual inspection was performed on each of the retrieved CALIPSO PBL heights. This was done for all of the data used in this study. Several subregions were chosen within the Western Hemisphere. Subregions were selected based on season and meteorological regimes; data were analyzed for August and December 2006. The GEOS-5 model data set available was limited when this research was conducted. August and December were selected to maximize the seasonal difference.

[15] PBL heights in Africa were also analyzed and compared. The area is bounded by the coordinates 35.0°N , 35.0°S , 45.0°W , 60.0°E (Figure 3). The analysis was performed from 8 to 18 August 2006, when biomass burning is the most intense in Southern Africa. Figure 4 displays the active fire pixels from the MODIS sensor for 18 August 2006. Burning occurs throughout the year in Africa due to farmers preparing for the agricultural season

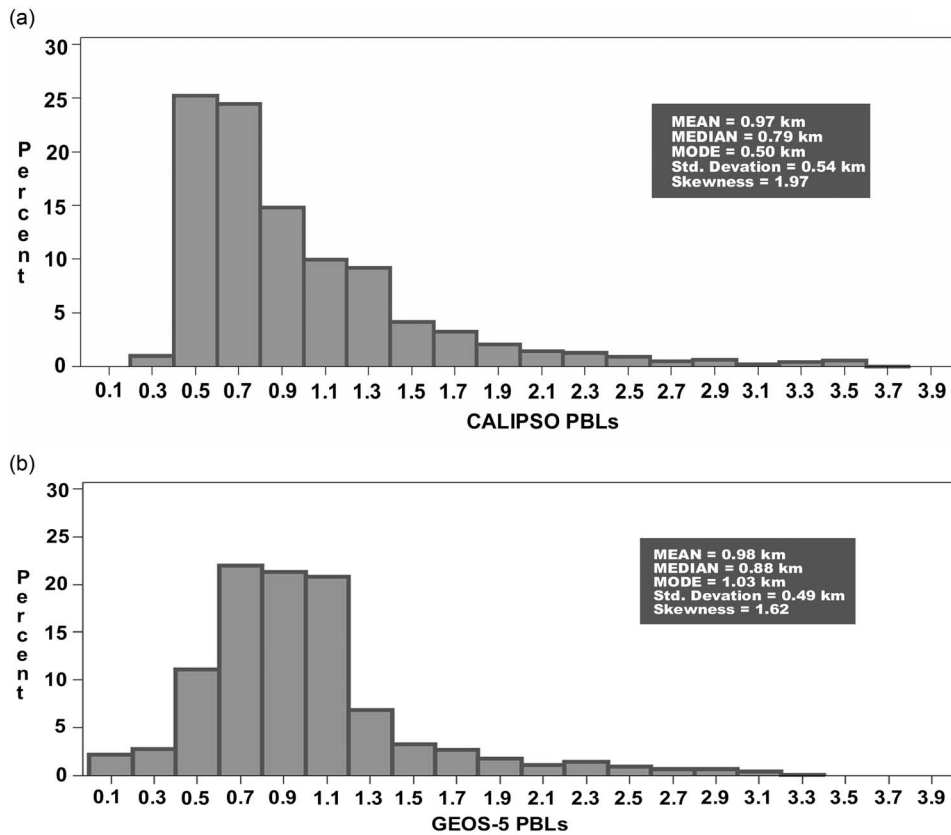


Figure 5. Histogram plots that show the CALIPSO and GEOS-5 PBL percent frequency for the month of August 2006.

and grazing areas. Burning also occurs at the end of the agricultural harvest. Thus, burning events are conducted based on the meteorological regimes of the continent

[Justice et al., 1996]. Many papers have been published that look at the release of smoke particles in this area [Justice et al., 1996; Ichoku et al., 2003; Ichoku and

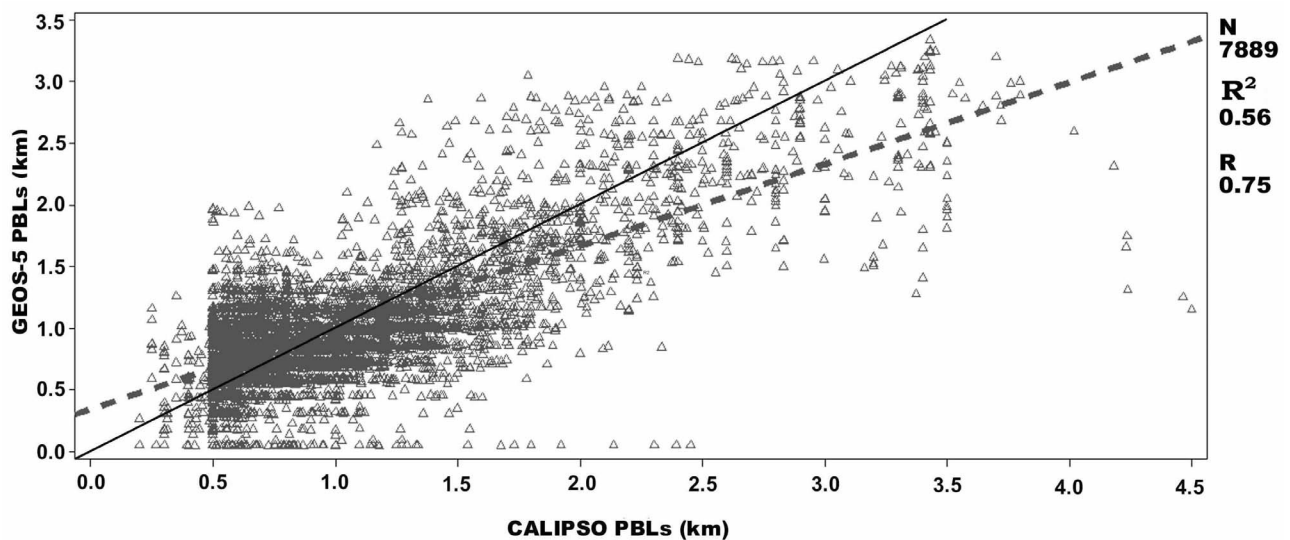


Figure 6. Correlation plot of GEOS-5 versus the CALIPSO PBL for August 2006. The coefficient of determination (R^2) is 0.56 and the correlation coefficient (R) is 0.75. Number of match-ups (N) is 7889, and the solid line is the one to one line. CALIPSO heights shown below 0.3 km were manually added in the QA process from obvious visual inspection of the data.

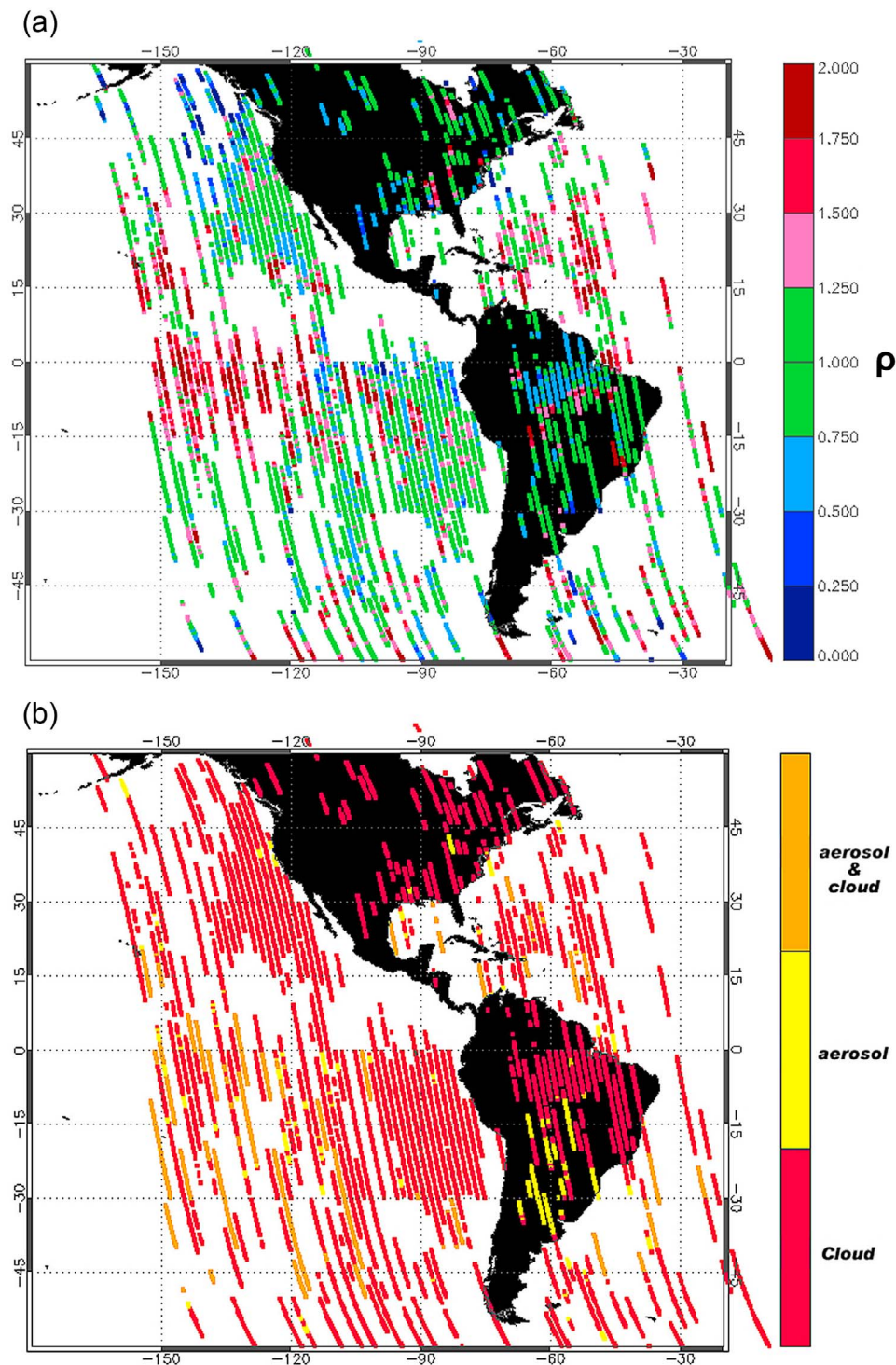


Figure 7. (a) Color-coded values of ρ for August 2006. Green values are $0.75 < \rho < 1.25$. (b) August 2006 flags which indicate the primary means of determining the PBL height from CALIPSO. Red, cloud used to determine the PBL height; yellow, top of aerosol layer is used; orange, the satellite PBL was derived via a combination of aerosol and cloud.

Kaufman, 2005; Matichuk et al., 2007]. All current smoke emission estimates have significant uncertainty errors [Andreae and Merlet, 2001; French et al., 2004; Jordan et al., 2008]. One contributing factor in the error of

smoke emission estimates can be attributed to the fact that scientists are not always sure of the relevant PBL height, which greatly impacts pollutant concentrations near the surface. The height of the PBL is important to

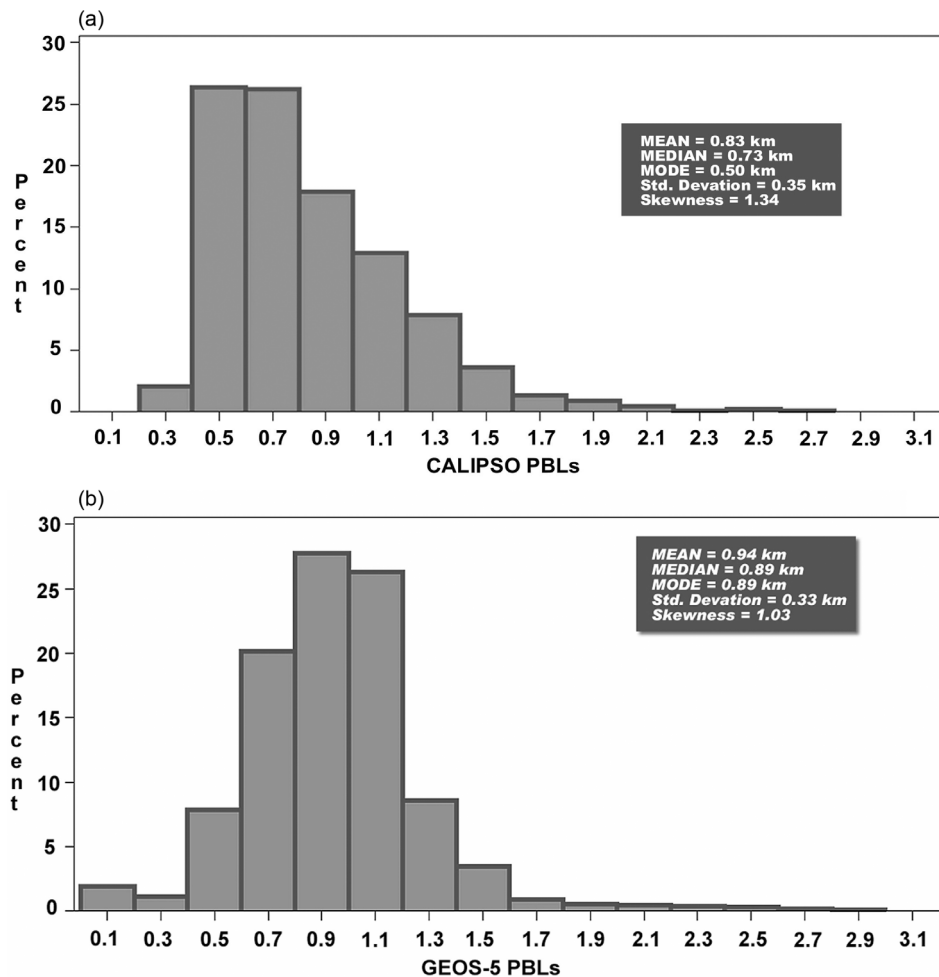


Figure 8. (a) Histogram plot that shows the CALIPSO PBL percentage frequency for the entire month of December 2006. (b) For the GEOS-5 model data set.

help researchers better understand smoke injection height as it relates to fire intensity.

4. Results

[16] Results are organized as follows: (1) the PBL heights derived from CALIPSO and GEOS-5 are presented in histogram charts which show the probability density function of PBL heights, (2) a correlation plot between the satellite and model PBL heights is given, (3) a ratio plot of the model estimate over the satellite observation is shown, and (4) a map of the flags which indicate the primary means to derive the PBL height from CALIPSO (via aerosol, cloud, or aerosol and cloud combined) is given.

4.1. Western Hemisphere; August 2006

[17] Figure 5a shows the distribution of the CALIPSO PBL height data. It is positively (right) skewed, which indicates that it has few large PBL values. Furthermore, the mean (0.97 km) is greater than the median (0.79 km) and mode (0.50 km). The most frequently occurring PBL height estimates range from 0.45 to 1.00 km. The GEOS-5 data (Figure 5b) is also positively skewed to the right but is not as extreme as the CALIPSO data set. The mean GEOS-5

PBL height is 0.98 km. The median and mode are 0.88 and 1.03 km, respectively.

[18] A correlation plot of the satellite versus the model PBL is shown in Figure 6. There were 7889 PBL match-ups between GEOS-5 and CALIPSO. The correlation coefficient is 0.75. Extreme outliers were mostly noted in cases where the model PBL height was significantly smaller than the satellite estimate. In most of these extreme daytime cases the model predicted a PBL height of 0.06 km (near the surface; lowest native vertical resolution level (i.e., 1) in GEOS-5), while most of the matched satellite PBLs varied from 0.50 to 2.50 km. There were few CALIPSO PBL instances less than 0.50 km because the algorithm started at 0.30 km to avoid land surface features around the globe. In most cases the SNR (signal-noise ratio) limitations of the CALIPSO daytime data make it very difficult to discern PBL heights below 500 m using the variance method. Strong attenuation of the daytime signal in the PBL has been recognized as a problem in the retrieval of extinction (M. Kacenelenbogen et al., An accuracy assessment of the CALIOP/CALIPSO version 2 aerosol extinction product based on a detailed multi-sensor, multi-platform case study, submitted to *Atmospheric, Physical and Chemical Discuss.*, 2010) leading to a number of artifacts in the CALIPSO near

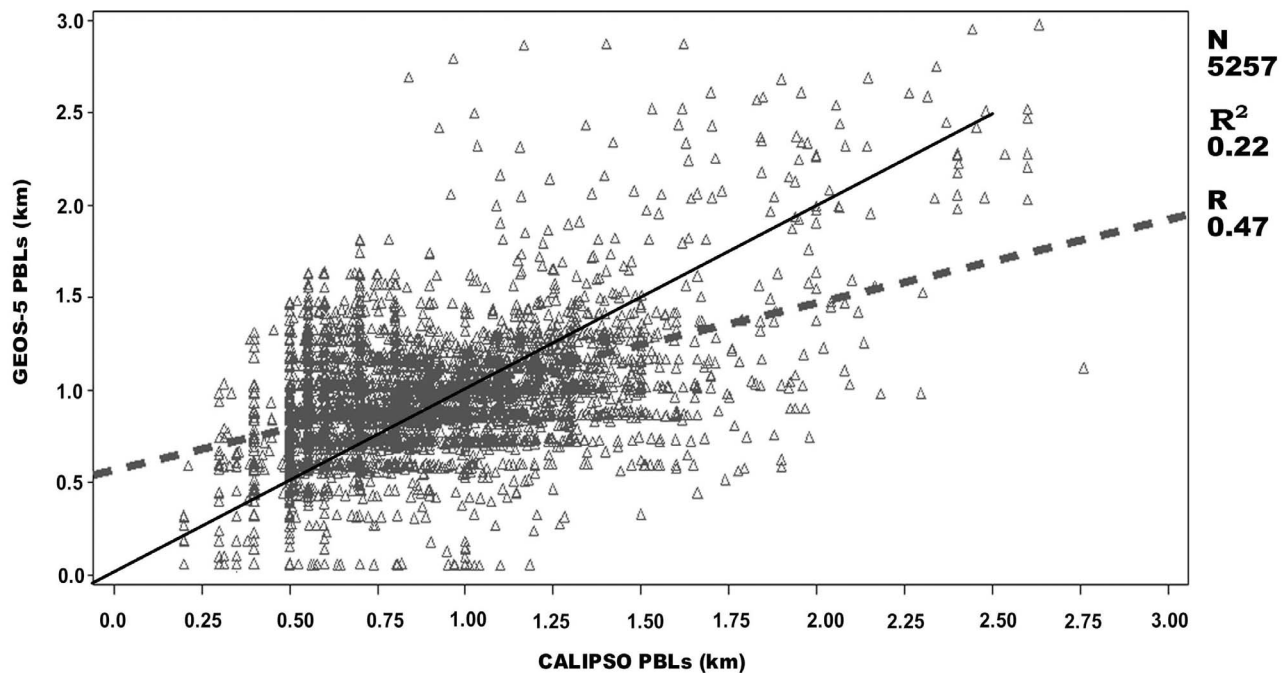


Figure 9. Correlation plot of GEOS-5 versus CALIPSO PBL. The correlation coefficient (R) is 0.47, and the black line is the one to one line.

surface data. We believe that this may have led to a similar artificial decrease in the number of PBL heights below 500 m in this study, which is a potential source of bias.

[19] A correlation plot of all the model and satellite match-ups is useful to identify variability in the data set. However, it is difficult to get a good understanding of where the outlying points lay on the globe. Each point on Figure 7a indicates the model/satellite PBL height ratio (ρ) relative to the same space and time. Moreover, green points are match-ups within 25% of unity (a perfect match between the model and satellite). Reddish points indicate cases where the model PBL was significantly greater (>25%) than that of the satellite estimate. Bluish points display cases where the model PBL was significantly lower than that of the CALIPSO estimate.

[20] The preponderance of green on the map (Figure 7a) indicates general approximate agreement between GEOS-5 and CALIPSO. The results displayed on the map reflect the correlation analysis (Figure 6). Underestimates (red points, $\rho < 0.75$) are mainly localized over water in the central equatorial Pacific. The PBL in this zone plays a key role in the coupled ocean-atmosphere dynamics that govern ENSO so that errors here are a concern. The fraction of low cloud and cloud radiative forcing in this zone are also overestimated in MERRA.

[21] Figure 7b shows the flag used based on the type of scattering to determine the PBL height from CALIPSO. Red dots in this figure indicate that clouds were used to decipher the PBL height from CALIPSO. Yellow dots indicate cases where the PBL height was derived from the top of a well-defined aerosol layer. Orange dots indicate cases where the satellite estimate was determined via well-defined mixed aerosol and cloud layer. For the Pacific near the equator, most of the CALIPSO PBL estimates determined from CALIPSO were determined by analyzing cloud layers

(indicated as red dots in Figure 7a over the Pacific region). Skin surface temperatures used in the GEOS-5 model were analyzed to determine if there might have been an overestimation in the model that could have led to the excessive larger than expected PBLH over the equatorial Pacific. Surface skin temperature measured by the Atmospheric Infrared Sounder (AIRS) [Tobin *et al.*, 2006] satellite was compared to surface temperatures from the GEOS-5 MERRA model to further investigate this.

[22] AIRS (Aqua) is part of the A-Train constellation and views the same region on Earth 75 s before CALIPSO. AIRS skin surface temperatures (daily AIRS Level-3 surface temperature product) from the ascending node were compared to the GEOS-5 skin surface. The mean skin surface temperature difference between AIRS and MERRA was found to be only 0.45°K with median of 0.51°K, not enough to change the height in the PBL over sea by a factor of 2.

[23] There are other disagreements between the model and satellite PBL estimates. A subregion worth highlighting in Figure 7a includes Central Brazil along the Amazon, where a swath of ρ less than 0.75 occurs. This case is analyzed in more detail by Jordan [2009]. Maps of precipitation correlate with the mismatch in PBL heights; however, we still do not have concrete evidence to explain the disagreements.

4.2. Western Hemisphere: December 2006

[24] The distribution of the PBLs derived via CALIPSO for December 2006 (Figure 8a) is also positively skewed similarly to the August 2006 data set. The mean PBL height derived from CALIPSO was 0.83 km. The median was 0.73 km, and mode was 0.50 km. However, the December data set is smaller (a difference of $N = 2632$ points) than August. This is because CALIPSO was not operating for

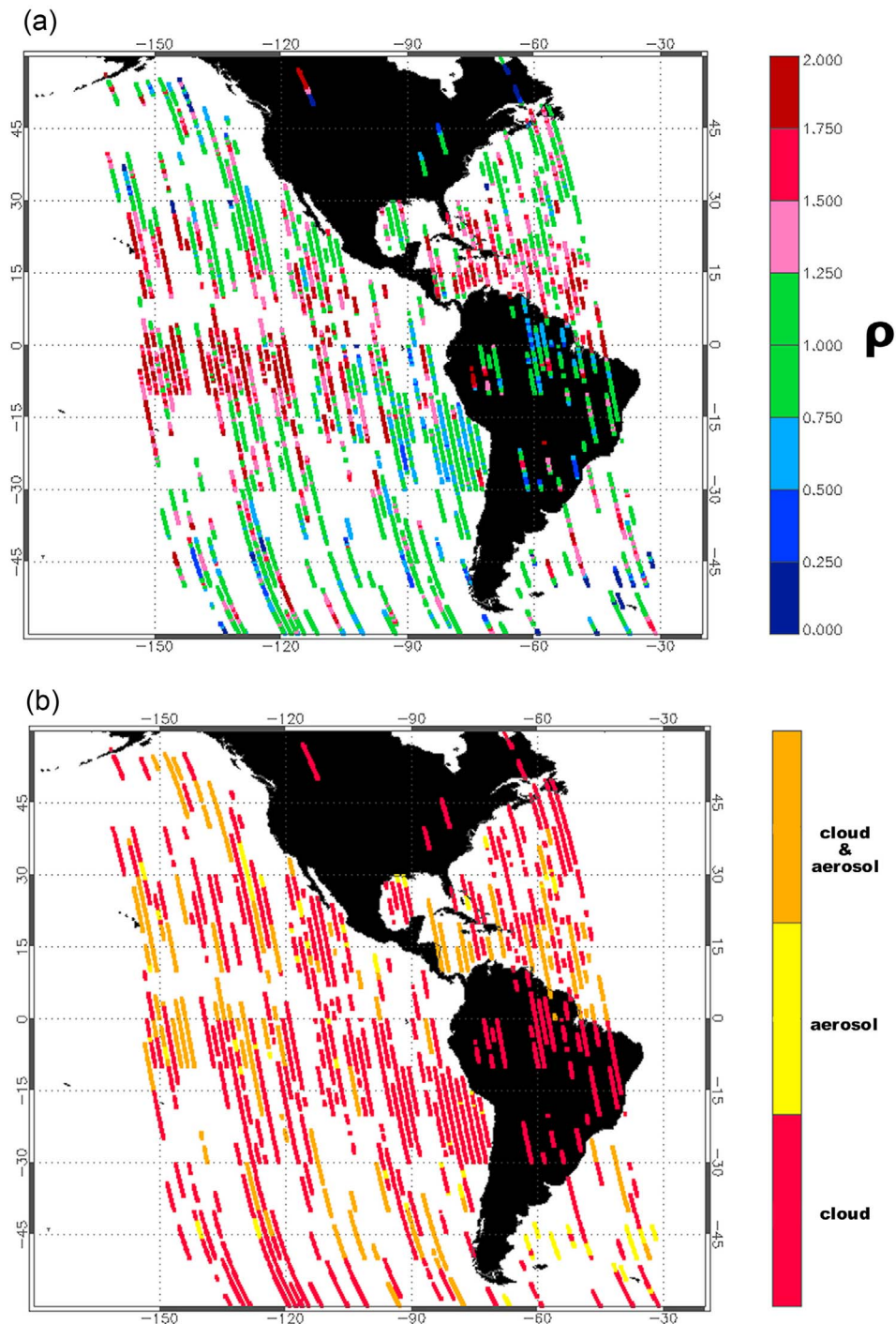


Figure 10. (a) The December 2006 satellite and model match-ups. Each point indicates the model/satellite ratio. Ratio points that were within 25% of unity are indicated in green. (b) The flags which indicate the primary means of determining the PBL height from CALIPSO.

10 days in December. Nevertheless, there are still a significant number of available points to conduct a statistical study. The GEOS-5 data (Figure 8b) is closer to a normal distribution. The summary statistics include a mean PBL height of 0.94 km and a 0.89 km median value. The mode is 0.89 km as well. Few instances exist where the model PBL was greater than 1.70 km.

[25] The December correlation plot of the model and satellite PBLs is shown in Figure 9. The correlation coefficient is 0.47. Extreme outliers were mostly noted in cases where the model PBL height was significantly greater than the satellite estimate. Most of these extreme cases were over the Equatorial Pacific region (Figure 10a) again, and for December, this predominates the points

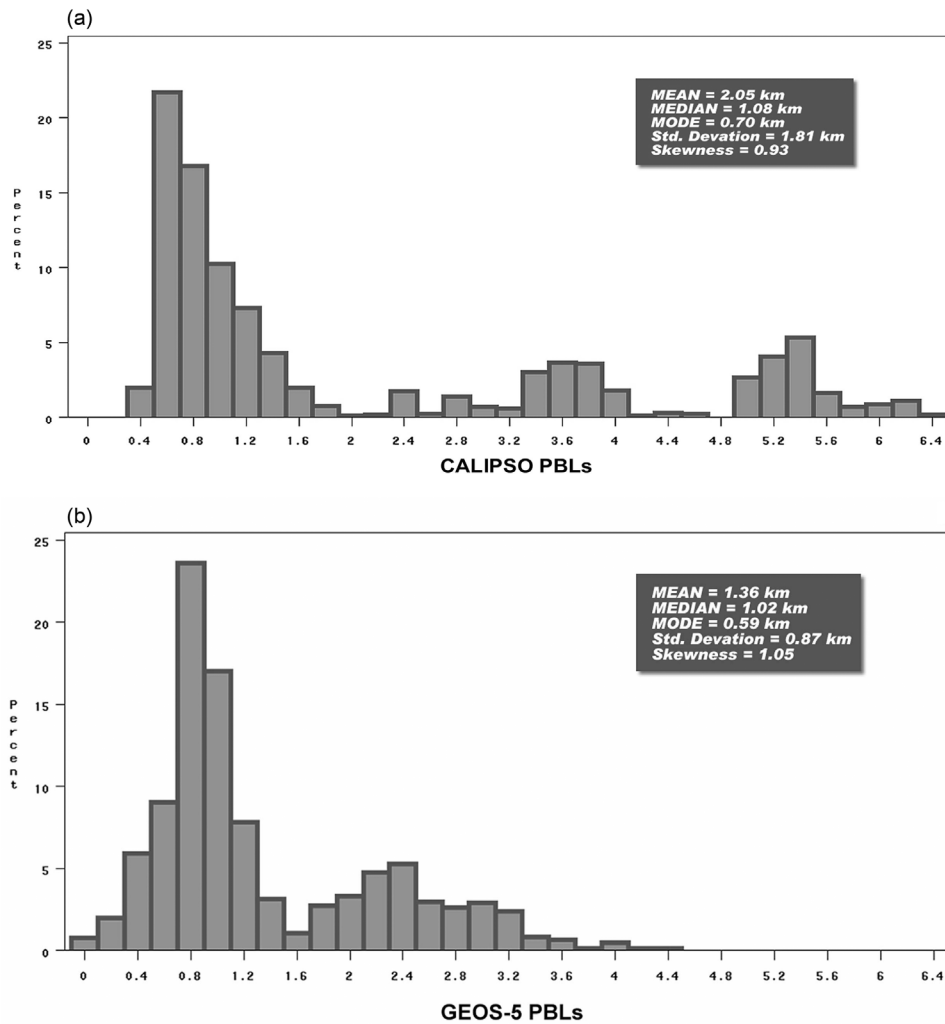


Figure 11. (a) Histogram plot which shows the CALIPSO PBL percent frequency for Africa (burning season) in August 2006. (b) For the GEOS-5 model data set.

responsible for the poorer correlation. Other noted outliers include cases where the model estimated a PBL height (~ 0.064 km) that was significantly lower than the satellite estimate. Furthermore, all of those cases were over water.

[26] There are more instances of $\rho > 1.25$ in the December 2006 (Figure 10a) data set than in August 2006 (Figure 7a). As in the August case, many of these instances occur over the equatorial Pacific. In the December data, there appears to be an increase in the number point with $\rho > 1.25$ in the Caribbean. Figure 10b displays the flag used to determine the PBL height from CALIPSO. Clouds were again the primary flag used in the December 2006 data set, but a larger proportion of cloud/aerosol flags are also evident compared with the August 2006 case (Figure 7b).

[27] An El Niño event was developing in December 2006 (NOAA NCEP CPC, <http://www.cpc.noaa.gov/>). It is expected that warmer equatorial Pacific SSTs associated with the El Niño event would drive greater than normal PBL heights over the equatorial Pacific. Seasonal cycle also has to be considered. August SSTs along the equatorial Pacific (150°W – 90°W) represent the coldest phase of

the normal annual cycle. For both reasons, we would expect higher PBLs in December 2006 than in August 2006. This was evident in the GEOS-5 model, PBL heights in GEOS-5 increased from ~ 0.6 to ~ 0.9 km in this zone; whereas in the CALIPSO data the increase was only from ~ 0.5 to ~ 0.6 km. The model's mean overprediction of PBL height in this region, as well as the apparent oversensitivity to SST may indicate a problem in its implementation of the *Lock et al.* [2000] scheme, or may indicate a bias in large scale descent over this region.

4.3. Africa Study Region

[28] The PBL height varied significantly across Africa (Figures 11a and 11b). The data set has three specific modes. The first and largest mode varied from 0.5 to 1.2 km in the satellite data set. The percent frequencies of the second and third modes were much smaller. The GEOS-5 model PBL data set had two modes. Summary statistics for both distributions are indicated on Figures 11a and 11b. The model data set had fewer instances of PBLs heights greater than 4 km (Figure 11b). PBL heights were higher where there was more burning activity (Figure 4). Determining the

August 2006 -Africa (Fire Season)

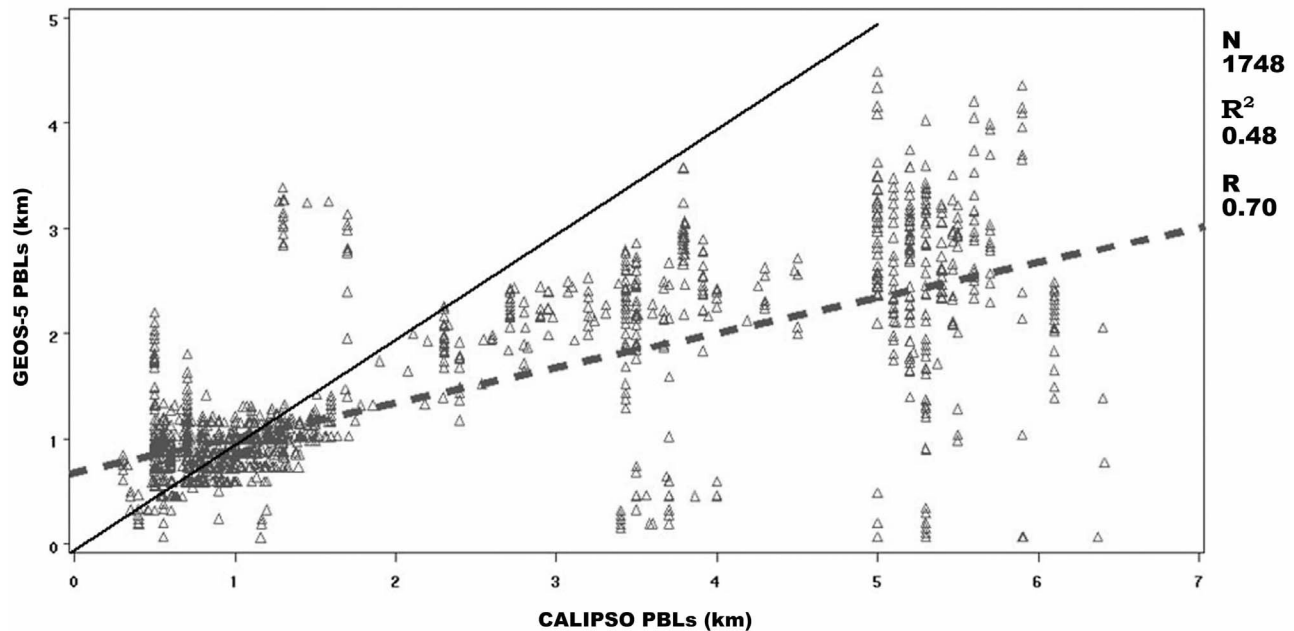


Figure 12. Correlation plot of GEOS-5 versus CALIOP PBL. The correlation coefficient (R) is 0.70, and the solid black line is the one to one line.

PBL height from CALIPSO was straightforward in these cases since the density of the aerosol layers were quite intense. One can clearly see where most of the aerosol was being capped, which flagged the height of the PBL. However, it is possible for intense fires to penetrate the PBL and loft to higher altitudes, leading to our overestimation of PBL heights. African savannah fires, however, are generally confined to the PBL. Another confounding factor could be the trapping of smoke within a residual layer from prior day PBL heating and long range transport to the CALIPSO overpass location. In most cases, aerosol and cloud layers were both well defined and were used to derive the PBL height from CALIPSO.

[29] The Africa August 2006 correlation plot (satellite versus model) is shown in Figure 12 and makes the three modes of data more obvious. The correlation coefficient is 0.70. The first mode corresponds to cases over the water. The second mode was related to cases over South Africa where, as shown in Figure 4, burning was prevalent. The third and final mode relates to cases over the Northern portion of Africa in the Sahara desert. Outliers were noted for all three modes. Extreme outliers were particularly obvious for larger PBL height cases in the Sahara desert. In these cases, the model PBL was less than 1 km while estimates from CALIPSO were greater than 3.3 km in altitude. Other noted outliers include cases where the model PBL (~ 3 km) was greater than the satellite estimate (~ 1.5 km).

[30] Each point on Figure 13a indicates the model/satellite ratio relative to the same space and no greater than 30 min in time. Most of the green points where $0.75 < \rho < 1.25$ were over (1) South Africa, (2) the South Atlantic Ocean, and (3) Indian Ocean. Several blue points that indicate cases where the model PBL was lower than the CALIPSO estimate are

mainly in Northern Africa where CALIPSOPBL heights ranged from 5 to 6.2 km. CALIPSO PBL heights ranged from 2.5 to 4.0 km over Southern Africa where burning was most intense. PBL heights derived from CALIPSO that were less than 1.5 km were primarily over water. Many red points, which indicate cases where the model PBL was significantly greater ($>25\%$) than the satellite estimate, were present over the Atlantic.

[31] Figure 13b graphically displays flags used to determine the PBL height from CALIPSO. Clouds were primarily used to determine the PBL height over the Southern Atlantic. Mostly aerosol layers were used to infer CALIPSO PBL heights over land.

5. Summary

[32] Climate modelers are constantly searching for new opportunities to verify model outputs. This is the first global observational study of PBL heights using CALIPSO with comparisons to the GEOS-5 MERRA model. Also, the present research provides better insight of PBL height variances in the GEOS-5 model.

[33] Two large regions were selected to derive PBL heights from CALIPSO. The largest region included most of the Western hemisphere. Africa was the second region studied. The analysis, for the first region, was performed for both August and December 2006. These months were selected since, at the time of writing, the available GEOS-5 MERRA data was limited and it was important to select months from different seasons.

[34] Satellite and model correlations were higher, on average ($R \sim 0.73$), for the August 2006 data sets (Africa and the Western half of the globe). Match-ups were not as

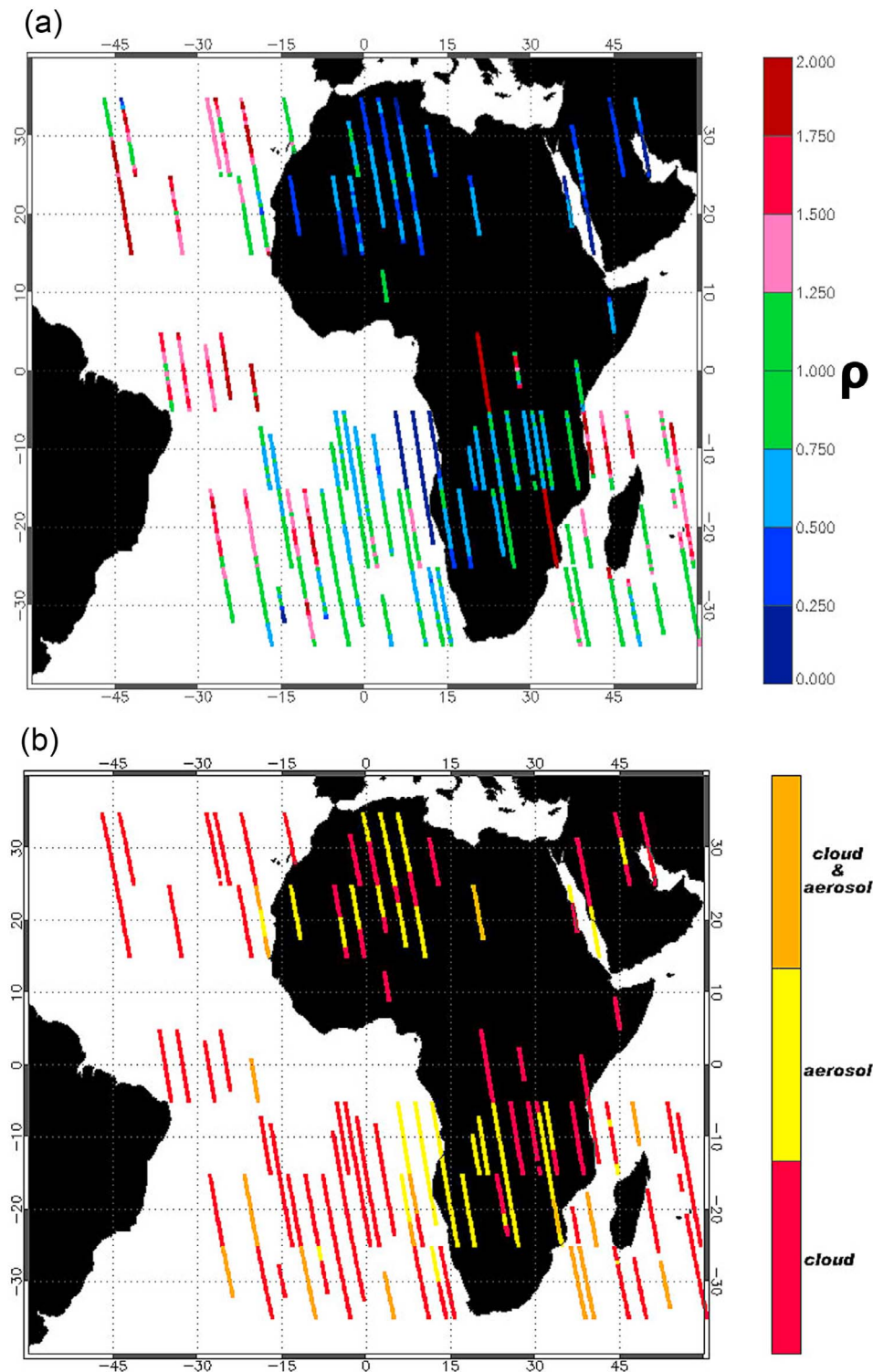


Figure 13. (a) The Africa August 2006 satellite and model match-ups. Each point indicates ρ or the model/satellite ratio. Ratio points that were within 25% of unity are indicated in green. (b) The flags that indicate the primary means of determining the PBL height from CALIPSO.

well correlated for the December 2006 data set ($R \sim 0.47$). It was evident that the model PBL height changed significantly when transitioning from land to water or from water to land.

[35] A significant disagreement between GEOS-5 PBL height and CALIPSO was noted over the equatorial Pacific, where model PBL heights were more than 25% greater than the CALIPSO satellite derived estimate. This may suggest

excessive forcing of turbulence by cloud top cooling in the GEOS-5 implementation of the Lock et al. PBL scheme.

[36] Our results also suggest significant disagreements in some land regions where wet surface conditions may exist (e.g., central Brazil) or where high surface temperatures exist (e.g., Saharan desert). There are indications that when an area has undergone recent precipitation the model PBL height deviates from what CALIPSO observes. There were cases over Northern Africa where the model PBL heights were much lower than the satellite-derived estimates. CALIPSO clearly observed well-defined aerosol and cloud layers up to 6 km in this area, but the model PBL was generally less than half of this value. It was also obvious that there were many instances where the CALIPSO derived PBL heights are generally higher, except for limited areas over the ocean, than the GEOS-5 model. It is important to note that most of the CALIPSO PBL heights were derived from cloudy data.

[37] **Acknowledgments.** This work was funded by Cooperative Center for Remote Sensing Science and Technology (CREST) CUNY grant 49100-00-02-B and NASA NAS1-99107.

References

- Andreae, M. O., and P. Merlet (2001), Emission of trace gases and aerosols from biomass burning, *Global Biogeochem. Cycles*, *15*, 955–966, doi:10.1029/2000GB001382.
- Arya, S. P. (1988), *Introduction to Micrometeorology*, Academic, San Diego, Calif.
- Bloom, S. C., L. L. Takacs, D. A. Silva, A. M., and D. Ledvina (1996), Data assimilation using incremental analysis updates, *Mon. Weather Rev.*, *124*, 1256–1271.
- Boers, R., and E. W. Eloranta (1986), Lidar measurements of the atmospheric entrainment zone and the potential temperature jump across the top of the mixed layer, *Boundary Layer Meteorol.*, *34*, 357–375.
- Bosilovich, M. G. (2008), NASA's modern era retrospective-analysis for research and applications: Integrating earth observations, *Earthzine*. (Available at <http://www.earthzine.org/2008/09/26/nasas-modern-era-retrospective-analysis>)
- Brooks, I. M. (2003), Finding boundary layer top: Application of a wavelet covariance transform to lidar backscatter profiles, *J. Atmos. Oceanic Technol.*, *20*, 1092–1105.
- Cohn, S. A., and W. M. Angevine (2000), Boundary-layer height and entrainment zone thickness measured by lidars and wind profiling radars, *J. Appl. Meteorol.*, *39*, 1233–1247.
- Davis, K. J., N. Gamage, C. R. Hagelberg, C. Kiemle, D. H. Lenschow, and P. P. Sullivan (2000), An objective method for deriving atmospheric structure from airborne lidar observations, *J. Atmos. Oceanic Technol.*, *17*, 1455–1468.
- French, N., P. Goovaerts, and E. S. Kasischke (2004), Uncertainty in estimating carbon emissions from boreal forest fires, *J. Geophys. Res.*, *109*, D14S08, doi:10.1029/2003JD003625.
- Ichoku, C., L. A. Remer, Y. J. Kaufman, R. Levy, D. A. Chu, D. Tanré, and B. N. Holben (2003), MODIS observation of aerosols and estimation of aerosol radiative forcing over southern Africa during SAFARI 2000, *J. Geophys. Res.*, *108*(D13), 8499, doi:10.1029/2002JD002366.
- Ichoku, C., and Y. J. Kaufman (2005), A method to derive smoke emission rates from MODIS fire radiative energy measurements, *IEEE Trans. Geosci. Remote Sens.*, *43*(11), 2636–2649.
- Jordan, N. S., C. Ichoku, and R. M. Hoff (2008), Estimating smoke emissions over the US Southern Great Plains using MODIS fire radiative power and aerosol observations, *Atmos. Environ.*, *42*, 2007–2022, doi:10.1016/j.atmosenv.2007.12.023.
- Jordan, N. S. (2009), Validation of the Version 5 Goddard Earth Observing System (GEOS-5) using Cloud-Aerosol Lidar and Infrared Pathfinder Satellite Observations (CALIPSO), Ph.D. dissertation, Univ. of Maryland, Baltimore County. (Available at http://alg.umbc.edu/3d-aqs/doc/Jordan_2009.pdf)
- Justice, C. O., J. D. Kendall, P. R. Dowty, and R. J. Scholes (1996), Satellite remote sensing of fires during the SAFARI campaign using NOAA advanced very high resolution radiometer data, *J. Geophys. Res.*, *101*(D19), 23,851–23,863, doi:10.1029/95JD00623.
- Justice, C. O., L. Giglio, S. Korontzi, J. Owens, J. T. Morissette, D. Roy, J. Descloitres, S. Alleaume, F. Petitcolin, and Y. Kaufman (2002), The MODIS fire products, *Remote Sens. Environ.*, *83*, 244–262.
- Lock, A. P., A. R. Brown, M. R. Bush, G. M. Martin, and R. N. B. Smith (2000), A new boundary layer mixing scheme: Part I. Scheme description and single column model tests, *Mon. Weather Rev.*, *128*, 3187–3199.
- Louis, J. F., M. Tiedtke, and J. F. Geleyn (1982), A short history of the operational PBL parameterization at ECMWF, in *Proceedings of ECMWF Workshop on PBL Parameterization*, ECMWF, Reading, UK.
- Maticuk, R. I., P. R. Colarco, J. A. Smith, and O. B. Toon (2007), Modeling the transport and optical properties of smoke aerosols from African savanna fires during the Southern African Regional Science Initiative campaign (SAFARI 2000), *J. Geophys. Res.*, *112*, D08203, doi:10.1029/2006JD007528.
- Melfi, S. H., J. Spinhirne, S.-H. Chou, and S. Palm (1985), Lidar observations of vertically organized convection in the planetary boundary layer over the ocean, *J. Clim. Appl. Meteorol.*, *24*, 806–824.
- Palm, S. P., D. Hagan, G. Schwemmer, and S. H. Melfi (1998), Inference of marine atmospheric boundary layer moisture and temperature structure using airborne lidar and infrared radiometer data, *J. Appl. Meteorol.*, *37*, 308–324.
- Palm, S. P., A. Benedetti, and J. Spinhirne (2005), Validation of ECMWF global forecast model parameters using GLAS atmospheric channel measurements, *Geophys. Res. Lett.*, *32*, L22S09, doi:10.1029/2005GL023535.
- Randall, D. A., Q. Shao, and M. Branson (1998), Representation of clear and cloudy boundary layers in climate models, in *Clear and Cloudy Boundary Layers*, edited by A. A. M. Holtslag and P. G. Duynkerke, pp. 305–322, Roy. Neth. Acad. Arts and Sci., Amsterdam.
- Rienecker, M. M., et al. (2008), The GEOS-5 Data Assimilation System—Documentation of Versions 5.0.1 and 5.1.0. NASA GSFC Technical Report Series on Global Modeling and Data Assimilation, vol. 27, pp. 92, *NASA/TM-2007-104606*.
- Stull, R. B. (1988), *An Introduction to Boundary Layer Meteorology*, 666 pp. Kluwer Acad., Norwell, Mass.
- Stull, R. B. (2000), *Meteorology for Scientists and Engineers*, Brooks/Cole, Pacific Grove, Calif.
- Tobin, D. C., H. E. Revercomb, R. O. Knuteson, B. M. Lesht, L. L. Strow, S. E. Hannon, W. F. Feltz, L. A. Moy, E. J. Fetzer, and T. S. Cress (2006), Atmospheric Radiation Measurement site atmospheric state best estimates for Atmospheric Infrared Sounder temperature and water vapor retrieval validation, *J. Geophys. Res.*, *111*, D09S14, doi:10.1029/2005JD006103.
- Winker, D. M., W. H. Hunt, and M. J. McGill (2007), Initial performance assessment of CALIOP, *Geophys. Res. Lett.*, *34*, L19803, doi:10.1029/2007GL030135.
- Winker, D. M., et al. (2010), The CALIPSO Mission: A global 3D view of aerosols and clouds, *Bull. Am. Meteorol. Soc.*, doi:10.1175/2010BAMS3009.1.

J. T. Bacmeister, National Center for Atmospheric Research, Climate and Global Dynamics Division, Boulder, CO, USA.

R. M. Hoff and N. S. Jordan, Joint Center for Earth Systems Technology, University of Maryland Baltimore County, Ste. 320, 5523 Research Park Dr., Baltimore, MD 21228, USA. (njordan1@umbc.edu)